Materials Letters 207 (2017) 66–71

Contents lists available at ScienceDirect

Materials Letters

journal homepage: www.elsevier.com/locate/mlblue

Highly stable silver nanoparticles synthesized using *Terminalia catappa* leaves as antibacterial agent and colorimetric mercury sensor

Aishwarya Devadiga, Vidya Shetty K.*, M.B. Saidutta

Department of Chemical Engineering, National Institute of Technology Karnataka, Surathkal, Srinivasnagar Post, Mangalore 575025, India

ARTICLE INFO

Article history:
Received 6 March 2017
Received in revised form 17 June 2017
Accepted 2 July 2017
Available online 5 July 2017

Keywords:
Antibacterial
Leaf extract
Mercury sensor
Silver nanoparticles
Terminalia catappa

ABSTRACT

Silver nanoparticles (AgNPs) were synthesized using the aqueous extract of an agrowaste: *Terminalia catappa* leaves. The AgNPs were characterized using UV–VIS spectroscopy, Transmission electron microscopy, Scanning electron microscopy, Fourier Transmission Infrared spectroscopy and Dynamic light scattering analysis. AgNPs were monodispersed, crystalline, quasi-spherical with average size of ~11 nm and were encapsulated with capping agents present in the extract. The AgNPs were stable with the zeta potential value of −36.7 mV. These AgNPs exhibited significant antibacterial activity against water borne pathogens and could be used as colorimetric sensors for the detection of trace levels of mercury, indicating their multifaceted application in antibacterial coating, water treatment and as colorimetric mercury sensors. The overall synthesis process emphasizes on the agrowaste utilization for the "green" synthesis of AgNPs.

1. Introduction

Silver nanoparticles (AgNPs) are highly sought after for the unique properties they exhibit at nanoscale level, thereby gaining scientific and industrial research attention for their application in fields pertaining to textile science [1,2], medicine, sensors and detectors [3], catalysis [4], supercapacitors [5], consumer products [6], data storage devices [7], disinfection and water treatment [8]. Synthesis of AgNPs using biobased routes has been rapidly gaining momentum as they overcome the demerits of chemical and physical synthesis routes, such as elevated process conditions and usage of toxic chemicals that are not environmentally benign. In the current research, leaves of *T. catappa* was chosen as the ideal source for the synthesis of AgNPs. These leaves are known to contain several bioactive components such as antioxidants, flavonoids like kaempferol, tannins, polyphenols and phenols [9–12] which remain unharnessed but can bring about the reduction of Ag^+ ions to Ag^0, leading to the formation of AgNPs [13–15]. The extract of *T. catappa* leaves have also been used for the synthesis of gold nanoparticles [16]. *T. catappa* leaves offer to be the better alternative bioresource for the synthesis of AgNPs as they do not carry any food and agro-economical value and also for channelling the bioactive components present in the waste biomass. In the present study, AgNPs have been successfully synthesized using the leaves of *T. catappa* leaves and evaluated for their application potential as antibacterial agents against water borne pathogens and as mercury sensors. This process of bio-based synthesis is benign, cost effective and is a green method of waste biomass utilization for the efficacious synthesis of AgNPs with application potential.

2. Materials and methods

2.1. Collection of the plant material and preparation of the aqueous leaf extract of T. catappa (ALE)

T. catappa leaves were collected from Surathkal, a town geographically positioned at 12°58′60 N 74°46′60E in Mangalore, India. Healthy leaves were collected, washed to eliminate dust; cut into small pieces. Further they were shade dried for 10 days and finely powdered. This leaf powder was used for the preparation of ALE. ALE was prepared by heating the leaf powder suspension consisting of 5 g of leaf powder in 100 mL of deionised water (5% w/v) through open solvent heating process till boiling and it was further allowed to boil for 5 min. The extract obtained was filtered through Whatman No.1 filter paper and was used for the synthesis of AgNPs.

2.2. Synthesis of AgNPs

The aqueous solution of silver nitrate ($AgNO_3$) with concentration of 20 mM was used as the precursor salt solution for the synthesis of AgNPs. The conditions for the synthesis of AgNPs have

* Corresponding author.
E-mail addresses: aishwarya.d.88@gmail.com (A. Devadiga), vidyaks68@yahoo.com, vidyaks95@nitk.ac.in (K. Vidya Shetty).

http://dx.doi.org/10.1016/j.matlet.2017.07.024
0167-577X/

been optimized earlier [17] and are used in the present work. ALE prepared with 5% leaf powder suspension and 20 mM $AgNO_3$ solution were made to react in 1:4 vol ratio with total volume of 10 mL at 28 ± 2 °C with an initial alkaline pH of 11 and under constant stirring for 24 h. The synthesis mixture was observed for the formation of brown colour as the preliminary confirmation, indicating the synthesis and presence of AgNPs in the colloidal solution. Spectral analysis of the synthesis mixture containing the AgNPs was performed using UV–VIS spectrophotometer (Labomed, USA) and the spectra were analyzed for the presence of surface plasmon resonance peak (SPR) for silver nanoparticles. Total flavonoid, antioxidant and total phenolic concentrations in the synthesis mixture before and after the AgNP synthesis were measured using the method described by Ordonez [18], Ferric Reducing Antioxidant power (FRAP) [19] assay and Folin-Ciocalteu method [20], respectively. The detailed methodology has been described in the Supplementary material Part A. The synthesis mixture containing AgNPs after the reaction time duration of 24 h, was centrifuged at 15,000 rpm for 10 min to separate the AgNPs and the supernatant was used for the determination of bioactive components. To determine the initial concentration of bioactive components in the synthesis mixture, 2 mL of the extract was diluted to 10 mL using deioninzed water and the sample was analyzed for the bioactive components. The separated nanoparticles were washed with deionised water to remove the contaminants and dried overnight at 130 °C in a hot air oven.

2.3. Characterization of the AgNPs

AgNPs were then characterized using X-Ray Diffraction analysis (XRD) (JEOL, Japan) to determine the crystallite size, Zetasizer SZ-100 (Horiba, USA) for particle size distribution analysis by Dynamic light scattering (DLS) and the zeta potential, Fourier Transform Infrared Spectroscopy (FTIR) (Avatar 360IR) and Transmission electron microscopic (TEM) (JEOL 2000 FX-II TEM, Japan) analysis.

2.4. Determination of antibacterial activity of AgNPs

The antibacterial property of the AgNPs was evaluated using well diffusion technique (provided as a Supplementary material Part B) by measuring the zone of inhibition (ZOI). Minimum inhibitory concentration (MIC) of the AgNPs against the test pathogens was determined using broth macrodilution method [21]. Culture strains of *E. coli* and *S. aureus* (Mc Farland 0.5 standard) were prepared. A stock suspension of AgNPs in Mueller Hilton broth was prepared with concentration of 102.4 μg/mL and was suitably diluted to prepare AgNP suspensions with concentrations ranging from 51.2 μg/mL to 0.2 μg/mL, for each of the test strains. The concentration of AgNPs at which no visual growth was observed after the incubation period (24 h) at 30 °C was determined as the MIC of AgNPs.

2.5. AgNPs as colorimetric sensors for mercury

The AgNPs were analyzed for their application as sensors to detect mercury levels in water. The colloidal solution of AgNPs of 0.1 mg/mL concentration was prepared with deionised water. 10 μL of 1 mg/mL mercuric chloride solution was added consecutively to 3 mL of the colloidal solution. The spectral analysis of this mixture containing the AgNPs and $HgCl_2$ after each addition of $HgCl_2$ solution was performed using UV–Vis spectrophotometer [22] and the presence of SPR peak and its intensity were noted. Addition of $HgCl_2$ was stopped when the colour of the reaction mixture turned colourless. AgNPs possess a characteristic deep brown colour in a colloidal form. After the addition of a particular amount of Hg^{2+}, the reaction mixture turned colourless.

3. Results and discussion

3.1. Synthesis and characterization of AgNPs

Preliminary confirmation of AgNP formation during the synthesis was provided by the visual observation of deep brown colour

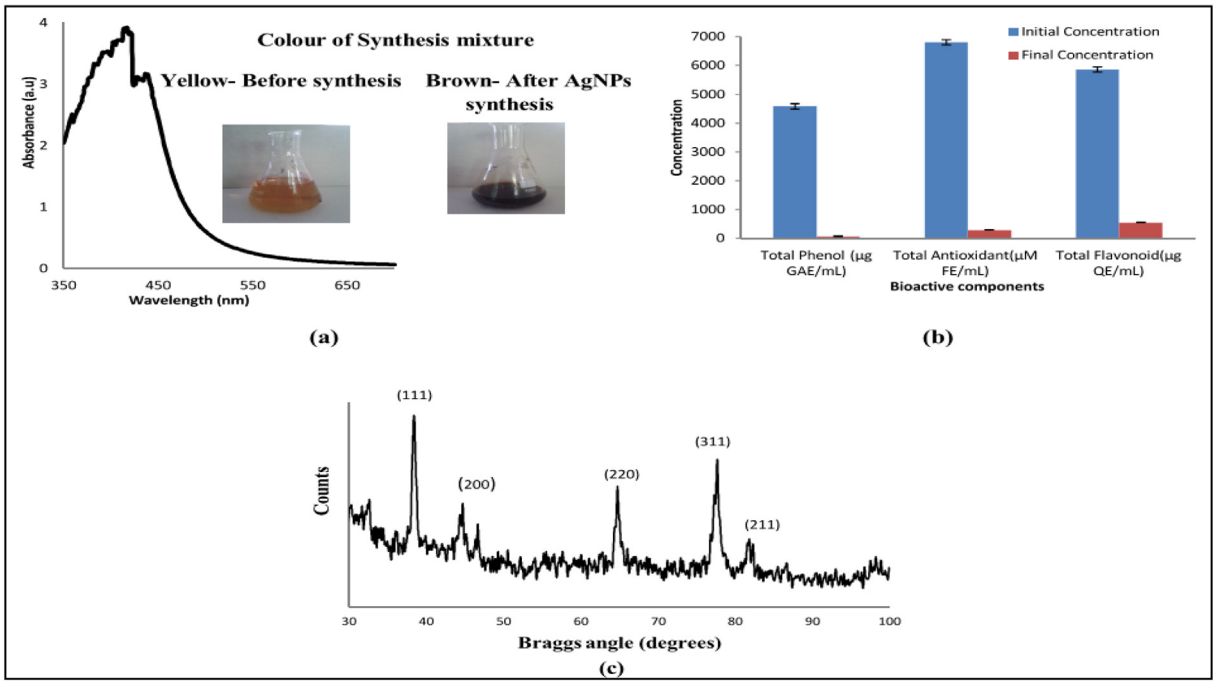

Fig. 1. (a) UV–VIS spectra showing the SPR peak characteristic of AgNPs (inset- Change in the colour of the synthesis mixture), (b) Total flavonoid, antioxidant and total phenolic content in the synthesis mixture before and after the synthesis of AgNPs using 5% ALE (c) XRD pattern of AgNPs showing the crystalline nature and the Millers indices of the AgNPs.

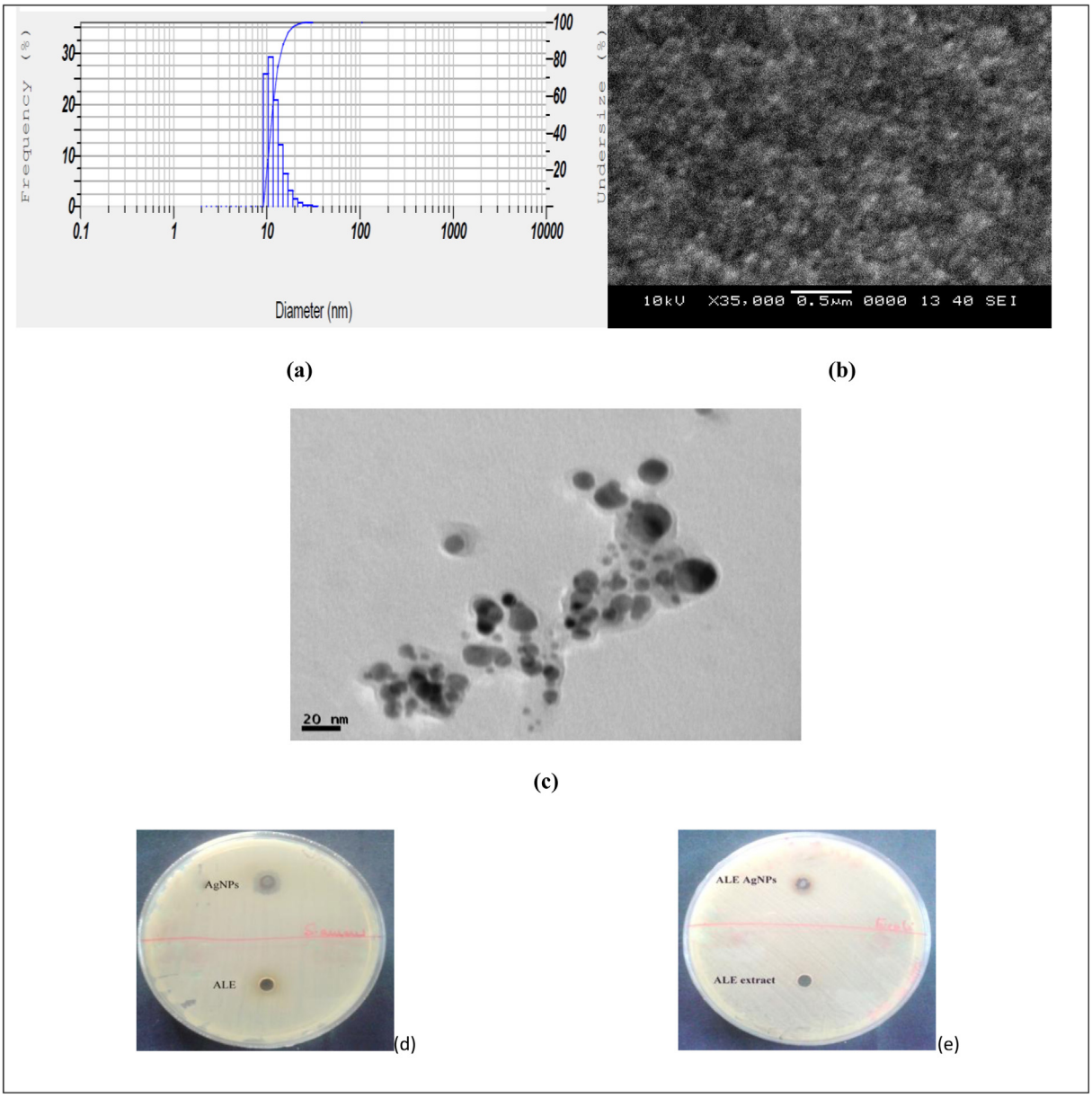

Fig. 2. (a) Particle size distribution (b) SEM image and (c) TEM image of AgNPs synthesized using ALE (d) ZOI of AgNPs against *E. coli* and (e) ZOI of AgNPs against *S. aureus*.

characteristic of AgNPs [23–25] in the synthesis mixture as shown in inset of Fig. 1(a). The SPR band of AgNPs as seen in Fig. 1(a) is sharp and intense with peak centred at 420 nm indicating the formation of a large number of monodispersed AgNPs. The split in the SPR peak indicates the difference in the energy levels of the longitudinal and transversal excitation modes of the AgNPs and the minimal distance of separation between these peaks indicates the formation of nearly isotropic AgNPs with a small deviation from perfectly spherical shape [26]. Fig. 1(b) shows that the total phenolics, flavonoid, and antioxidant content in the synthesis mixture reduced considerably after the synthesis of AgNPs, indicating that these plant bioactive components act as reducing and capping agents. X-ray Diffractogram of the AgNPs in Fig. 1(c) revealed the crystalline nature and the face centred cubic structure of metallic silver (JCPDS File No-04-0783) with peaks belonging to (1 1 1), (2 0 0), (2 2 0), (3 1 1) and (2 1 1) planes. The average crystallite size of AgNPs was determined using DeBye-Scherrer's formula and was found to be 8.27 nm.

The particle size distribution analysis of AgNPs as seen in Fig. 2 (a) revealed that the size of AgNPs lie in the range of 9–35 nm with an average size of 10.9 nm. The narrow size range indicates the presence of fairly monodispersed AgNPs and the average size obtained is almost similar to the crystallite size obtained through XRD analysis. The zeta potential value of AgNPs was found to be −36.7 mV indicating good stability in water as a solvent. FTIR spectrum of AgNPs (provided as a Supplementary material–Part C) exhibited a strong peak at 3609 cm^{-1} belonging to N—H group stretching vibrations [27], peaks from 3991 cm^{-1} to 3609 cm^{-1} belonging to —C— vibration of the carboxylic group; the peaks occurring at 3451 cm^{-1} belonging to the vibration of O—H groups of phenols, the peak at 3364 cm^{-1} of the N—H group from the peptides and at 2931.6 cm^{-1} belonging to asymmetric stretching of C—H bonds, peaks centred around 2114 cm^{-1} belonging to the C═C variables, while the groups belonging to carboxylic acid (C═O) are indicated by a peak at 1740.7 cm^{-1} and 1366.2 cm^{-1} [28,29]. The peaks at 1639.8 cm^{-1}, 1510.8 cm^{-1} and 1215.9 cm^{-1}

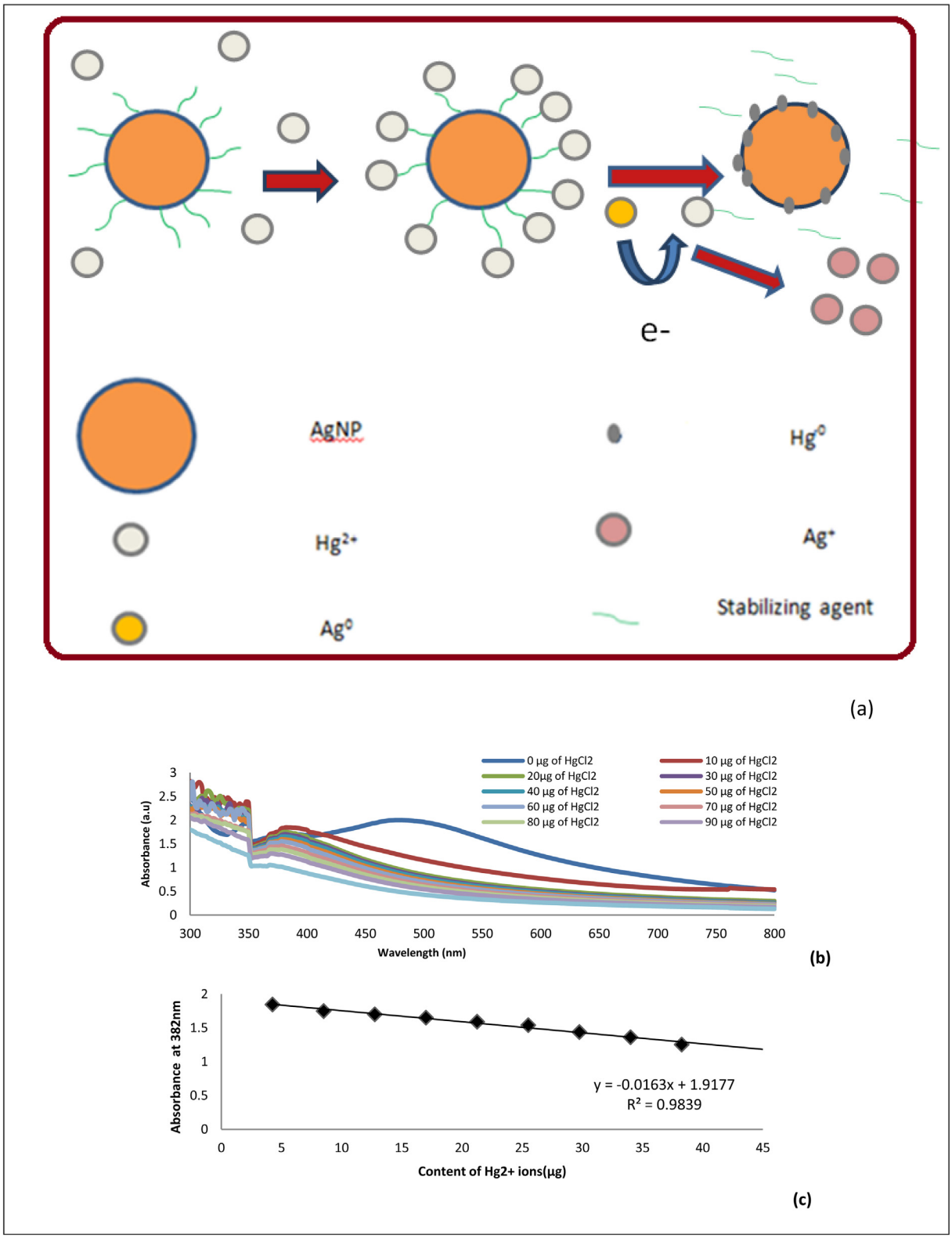

Fig. 3. (a) Schematic representation of the mercury sensing mechanism of AgNPs (b) SPR peaks obtained after addition of mercury to the colloidal suspension of AgNPs (c) Absorbance at 382 nm with different amount of mercury added to the colloidal suspension of the AgNPs showing linearity.

indicate the presence of aromatic rings, amine groups and polyol groups respectively [30]. These results confirm the presence of various organic groups on the surface of the AgNPs and thus indicate the role of plant bioactive components encapsulating the AgNPs as capping agents.

SEM and TEM analysis in Fig. 2(b) and (c) reveals the formation of quasi-spherical shaped AgNPs with size ranging from 4.56 nm to 20 nm and an average size of 10.56 nm (Image J software, Number of nanoparticles considered for size calculation is 48). Narrow size range confirms monodispersed nature of AgNPs. The presence of

capping around the nanoparticles is evident in the TEM image (Fig. 2(c)), showing that the AgNPs are encapsulated in a layer formed by the capping agents in ALE.

3.2. Antibacterial activity of AgNPs

Previous literature reports have demonstrated antibacterial activity of AgNPs [31,32]. A ZOI of 20 mm and 14 mm against *S. aureus* and *E. coli* were observed respectively, in the plates after incubation around the wells containing the AgNPs, as seen in Fig. 2(d) and (e) indicating the antibacterial effect of these AgNPs. ZOI with the extract was very less as compared to AgNPs as shown in Fig. 2(d) and (e). 25.6 μg/mL of AgNPs was determined as the MIC value for both *S. aureus* and *E. coli*, as no visible bacterial growth was observed above this concentration. Low MIC values ascertain that these AgNPs exhibit good antibacterial property.

3.3. Mercury sensing property of AgNPs synthesized using ALE

The mercury sensing property of AgNPs was evaluated using the methodology described in Section 2.5. The addition of $HgCl_2$ solution caused a characteristic decrease in the absorption intensity of the SPR peak and blue shift of the spectra was observed as shown in Fig. 3(b). This decrease in the absorption intensity and blue shift of the spectra can be explained by the redox reaction taking place at the surface of the AgNP, owing to the differences in the standard potential of 0.8 V (Ag^+/Ag) and 0.85 V (Hg^{2+}/Hg) [33]. Mercury (II) ions are colourless in solutions owing to a closed-shell d^{10} configuration and no optical spectroscopic signature [22], while AgNPs exhibit characteristic brown colour. When $HgCl_2$ is added to the colloidal AgNP suspension, the presence of organic capping agents on the surface of AgNPs promotes electrostatic–ionic attractions between the nanoparticle surface and mercury ions [34,35]. The mercury added, removes the stabilizing agents present on the surface of the AgNPs, on reacting with the Ag core by a Redox reaction [22], as shown in the schematic representation of the mechanism of AgNPs acting as sensors for the detection of mercury in Fig. 3 (a). Hg^{2+} forms organo metallic complexes on the surface of AgNPS, as the organic moieties in the capping render the required functional groups. Flavonoids and polyphenolic compounds such as gallic acid, catechol, pyrogallol, and their derivatives are present in plant extracts [36,37] and are known to form complexes with heavy metal cations [38–42]. These compounds in the plant extract provide metal interacting multi-functional groups such as hydroxyl, carboxyl and hetero-aromatic rings [38,41] on the AgNP capping [33,42]. Yang et al. [43] have also reported that organic phenolic ligands exhibit versatile coordination behaviour with different metal ions. These phenolic ligands in the capping of AgNPs would provide metal ions interacting surface functionality for developing selective colorimetric sensor for toxic metal ions [44]. Thus, the presence of organic functional groups in the capping facilitate the binding of mercury on to the surface of silver nanoparticles. Further, these capping agents which majorly have antioxidant properties serve as reducing agents and reduce Hg^+ ions to Hg^0 [45]. Thus, these redox reactions lead to removal of capping agents from the surface. Hg^{2+} gets reduced to Hg^0 on the surface of AgNPs, while oxidizing zerovalent silver (Ag^0) on the surface to Ag^+ ions [22]. The size of AgNPs reduces as AgNPs react with Hg^{2+} to form Ag^+. Hg^0 forms tiny Hg-Ag colloidal amalgams with AgNPs, The Hg-Ag amalgam forms a coating on the surface of AgNPs thus changing the colour of the colloidal solution. As the AgNPs are converted to Ag^+ ions by Hg^{2+}, the colloidal solution becomes colourless, indicating that the available Ag^0 in the colloidal suspension has been completely oxidized by the added quantity of mercury. Several reports pertaining to the use of AgNPs as sensors are available wherein the surface of the synthesized AgNPs was functionalized by addition of other molecules. In the present research work, the AgNPs were used as synthesized with no modification of the surface. The functionalization of the AgNP surface occurs during the synthesis process itself by the plant bioactive components, leading to an eco-friendly approach for selective mercury sensing.

The plot in Fig. 3(c) is linear with the negative slope indicating a decrease in absorbance with increase in Hg^{2+} content. It is one of the crucial mandates, that a sensing element should provide linearity between its input variable and the output variable for any inference or the measurement application. Fig. 3(c) shows a linearity between the Hg^{2+} ion level (input variable) and the absorbance (output variable), thus implying the suitability of AgNP based sensing method for Hg^{2+} detection and concentration measurement. The maximum detectable level was determined by the addition of Hg^{2+} ions to the colloidal solution till the solution turned colourless and no SPR peak was observed, while the minimum detectable level was determined by the maximum amount of Hg^{2+} ions added to the AgNPs colloidal solution that resulted in decrease in the intensity of SPR peak with a prominent blue shift. The maximum and minimum detectable concentration for Hg^{2+} ions with 0.3 mg of AgNPs (0.1 mg/mL) was found to be 12.75 μg/mL and 0.85 μg/mL respectively.

4. Conclusion

A simple, benign and rapid process of biosynthesizing metallic AgNPs using an agrowaste, *T. catappa* leaves under ambient conditions of synthesis was successfully accomplished. The AgNPs were monodispersed, quasi-spherical shaped and with an average size of ~11 nm, with capping agents present on their surface which imparted stability to the AgNPs. These AgNPs exhibited significant antibacterial activity against water borne pathogens and good mercury sensing property. Thus, the AgNPs synthesized using ALE exhibit promising potential as antibacterial agents and mercury sensors. The antibacterial efficacy of these AgNPS may find suitable applications in the field of water treatment, antibacterial textile and the mercury sensing property may find application in determination of trace mercury pollution level in various ecosystems or comestibles. The overall process offers an advantage in utilization of the agro-waste generated in surplus amounts for the "green" synthesis of AgNPs with negligible chemical footprint on the environment.

Appendix A. Supplementary data

Supplementary data associated with this article can be found, in the online version, at http://dx.doi.org/10.1016/j.matlet.2017.07.024.

References

[1] M. Satio, Antibacterial, deodorizing, and UV absorbing materials obtained with zinc oxide (ZnO) coated fabrics, J. Coated Fabr. 23 (1993) 150–164.
[2] H.J. Lee, S.H. Jeong, Bacteriostasis and skin innoxiousness of nanosize silver colloids on textile fabrics, Text. Res. J. 75 (2005) 551–556.
[3] S. Silver, L.T. Phung, G. Silver, Silver as biocides in burn and wound dressings and bacterial resistance to silver compounds, J. Ind. Microbiol. Biotechnol. 33 (2006) 627–634.
[4] C. Vaseashta, D. Dimova-Malinovska, Nanostructured and nanoscale devices, sensors and detectors, Sci. Technol. Adv. Mater. 6 (2005) 312–318.
[5] L. Shen, L. Du, S. Tan, Z. Zang, C. Zhao, W. Mai, Flexible electrochromic supercapacitor hybrid electrodes based on tungsten oxide films and silver nanowires, Chem Commun. 52 (2016) 6296–6299.
[6] S. Kokura, O. Handa, T. Takagi, T. Ishikawa, Y. Naito, T. Yoshikawa, Silver nanoparticles as a safe preservative for use in cosmetics, Nanomed. Nanotechnol. Biol. Med. 6 (2010) 570–574.

[7] H. Ditlbacher, J.R. Krenn, B. Lamprecht, A. Leitner, F.R. Aussenegg, Spectrally coded optical data storage by metal nanoparticles, Opt. Lett. 25 (2000) 563–565.
[8] P. Jain, T. Pradeep, Potential of silver nanoparticle-coated polyurethane foam as an antibacterial water filter, Biotechnol. Bioeng. 90 (2005) 59–63.
[9] T.F. Ko, Y.M. Weng, Y.Y. Chiou, Squalene content and antioxidant activity of *Terminalia catappa* leaves and seeds, J. Agric. Food Chem. 50 (2002) 5343–5348.
[10] M.S. Owolabi, O.A. Lawal, I.A. Ogunwande, R.M. Hauser, W.N. Setzer, Chemical composition of the leaf essential oil of *Terminalia catappa* L. growing in Southwestern Nigeria, J. Essent. Oils Nat Prod. 1 (2013) 51–54.
[11] C.C. Chyau, S.Y. Tsai, P.T. Ko, J.L. Mau, Antioxidant properties of solvent extracts from *Terminalia catappa* leaves, Food Chem. 78 (2002) 483–488.
[12] J.L. Mau, P.T. Ko, C.C Chyau, Aroma characterization and antioxidant activity of supercritical carbon dioxide extracts from *Terminalia catappa* leaves, Food Res. Int. (2003) 3697–4104.
[13] H.M. El-Rafie, M.A.A. Hamed, Antioxidant and anti-inflammatory activities of silver nanoparticles biosynthesized from aqueous leaves extracts of four Terminalia species, Adv. Nat. Sci. Nanosci. Nanotechnol. 5 (2014) 035008.
[14] V. Singh, A. Shrivastava, N. Wahi, Biosynthesis of silver nanoparticles by plants crude extracts and their characterization using UV, XRD TEM and EDX, Afr. J. Biotechnol. 14 (2015) 2554–2567.
[15] A. Devadiga, K.V. Shetty, M.B. Saidutta, Effect of precursor salt solution concentration on the size of silver nanoparticles synthesized using aqueous leaf extracts of T. catappa and T. grandis Linn f.—a green synthesis route, in: Materials, Energy and Environment Engineering, Springer, Singapore, 2017, pp. 145–151.
[16] B. Ankamwar, Biosynthesis of gold nanoparticles (green-gold) using leaf extract of Terminalia Catappa, E-J. Chem. 7 (2010) 1334–1339.
[17] A. Devadiga, Biobased Synthesis of Silver and Titanium Dioxide Nanoparticles and Their Applications (Ph.D. thesis), National Institute of Technology Karnataka, Surathkal, 2016.
[18] A.A.L. Ordonez, J.D. Gomez, M.A. Vattuone, Antioxidant activities of *Sechium edule* (Jacq.) Swartz extracts, Food Chem. 97 (2006) 452–458.
[19] I.F. Benzie, J.J. Strain, The ferric reducing ability of plasma (FRAP) as a measure of "antioxidant power": the FRAP assay, Anal. Biochem. 239 (1996) 70–76.
[20] V.L. Singleton, R. Orthofer, R.M. Lamuela-Raventos, Analysis of total phenols and other oxidation substrates and antioxidants by means of folin-ciocalteu reagent, Methods Enzymol. 299 (1999) 152–178.
[21] G. Huys, Antibiotic Susceptibility Testing of Aquaculture Associated Bacteria with the Broth Macrodilution Method (MIC Determination) SOP ASIARESIST, Laboratory of Microbiology, Universiteit Gent, K.L. Ledeganckstr. 35, B-9000 Gent, Belgium.
[22] K. Farhadi, M. Forough, R. Molaei, S. Hajizadeh, A. Rafipour, Highly selective Hg^{2+} colorimetric sensor using green synthesized and unmodified silver nanoparticles, Sens. Actuators, B 161 (2012) 880–885.
[23] S. Basavaraja, S.D. Balaji, A. Lagashetty, A.H. Rajasab, A. Venkataraman, Extracellular biosynthesis of silver nanoparticles using the fungus *Fusarium semitectum*, Mater. Res. Bull. 43 (2008) 1164–1170.
[24] J.Y. Song, B.S. Kim, Rapid biological synthesis of silver nanoparticles using plant leaf extracts, Bioprocess. Biosyst. Eng. 32 (2009) 79–84.
[25] B.S. Maria, A. Devadiga, V.S. Kodialbail, M.B. Saidutta, Synthesis of silver nanoparticles using medicinal Zizyphus xylopyrus bark extract, Appl. Nanosci. (2014) 1–8.
[26] D.D. Evanoff Jr., G. Chumanov, Size-controlled synthesis of nanoparticles. "Silver-Only" aqueous suspensions via hydrogen reduction, J. Phys. Chem. B 108 (2004) 13957–13962.
[27] S. Ashokkumar, S. Ravi, V. Kathiravan, S. Velmurugan, Synthesis, characterization and catalytic activity of silver nanoparticles using Tribulus terrestris leaf extract, Spectrochim. Acta A 121 (2014) 88–93.
[28] K.B. Narayanan, N. Sakthivel, Biological synthesis of metal nanoparticles by microbes, Adv. Colloid Interface Sci. 156 (2010) 1–13.
[29] D. Philip, Green synthesis of gold and silver nanoparticles using Hibiscus rosa sinensis, Physica E 42 (2010) 1417–1424.
[30] V. Bansal, D. Rautaray, A. Bharde, Fungus-mediated biosynthesis of silica and titania particles, J. Mater. Chem. 15 (2005) 2583–2589.
[31] T. Suwatthanarak, B. Thanardna, D. Danwanichaul, P. Danwanichakul, Synthesis of silver nanoparticles in skim natural rubber latex at room temperature, Mater. Lett. 168 (2016) 31–35.
[32] M.J. Ahmed, G. Murtaza, A. Mehmood, T.M. Bhatti, Green synthesis of silver nanoparticles using leaves extract of *Skimmia laureola*: Characterization and antibacterial activity, Mater. Lett. 153 (2015) 10–13.
[33] S.S. Ravi, L.R. Christena, N. SaiSubramanian, S.P. Anthony, Green synthesized silver nanoparticles for selective colorimetric sensing of Hg^{2+} in aqueous solution at wide pH range, Analyst 138 (2013) 4370–4377.
[34] T. Pradeep, Noble metal nanoparticles for water purification: a critical review, Thin Solid Films 51 (2009) 6441–6478.
[35] K.V. Katok, R.L. Whitby, T. Fukuda, T. Maekawa, I. Bezverkhyy, S.V. Mikhalovsky, A.B. Cundy, Hyperstoichiometric interaction between silver and mercury at the nanoscale, Angew. Chem. Int. Ed. 51 (2012) 2632–2635.
[36] B. Sumi Maria, A. Devadiga, K.V Shetty, M.B. Saidutta., Solar photocatalytically active, engineered silver nanoparticle synthesis using aqueous extract of mesocarp of *Cocos nucifera* (Red Spicata Dwarf), J. Exp. Nanosci. 12 (2017), http://dx.doi.org/10.1080/17458080.2016.1251622.
[37] A. Devadiga, K.V. Shetty, M.B. Saidutta, Timber industry waste-teak (Tectona grandis Linn.) leaf extract mediated synthesis of antibacterial silver nanoparticles, Int. Nano Lett. 5 (2015) 205–214.
[38] M. McDonald, I. Mila, A. Scalbert, Precipitation of metal ions by plant polyphenols: optimal conditions and origin of precipitation, J. Agric. Food Chem. 44 (1996) 599–606.
[39] D.G. Strawn, D.L. Sparks, Effects of soil organic matter on the kinetics and mechanisms of Pb(II) sorption and desorption in soil, Soil Sci. Soc. Am. J. 64 (2000) 144–156.
[40] S. Kraemer, J. Xu, K. Raymond, G. Sposito, Adsorption of Pb(II) and Eu(III) by oxide minerals in the presence of natural and synthetic hydroxamate siderophores, Environ Sci. Technol. 36 (2002) 1287–1291.
[41] E. Giannakopoulos, P. Stathi, K. Dimos, D. Gournis, Y. Sanakis, Y. Deligiannakis, Adsorption and radical stabilization of humic-acid analogues and Pb2+ on restricted phyllomorphous clay, Langmuir 22 (2006) 6863–6873.
[42] D. Karthiga, S.P. Anthony, Selective colorimetric sensing of toxic metal cations by green synthesized silver nanoparticles over a wide pH range, RSC Adv. 3 (2013) 16765–16774.
[43] X. Yang, J.D. Ranford, J.J. Vittal, Isomerism in 1D coordination polymers of Cu (II) complexes of N-(2-hydroxybenzyl)-l-valine: influence of solvent and coordination sphere on the conformation, Cryst. Growth Des. 4 (2004) 781–788.
[44] V. Vinod, S.P. Kumar, Anthony, Silver nanoparticles based selective colorimetric sensor for Cd2+, Hg2+ and Pb2+ ions: tuning sensitivity and selectivity using co-stabilizing agents, Sens. Actuators, B 191 (2014) 31–36.
[45] C.Y. Lin, C.J. Yu, Y.H. Lin, W.L. Tseng, Colorimetric sensing of silver(I) and mercury(II) ions based on an assembly of Tween 20-stabilized gold nanoparticles, Anal. Chem. 82 (2010) 6830–6837.